Journal of Multiscale Modelling
Vol. 6, No. 2 (2015) 1550003 (12 pages)

DOI: 10.1142/S1756973715500031

Imperial College Press
www.icpress.co.uk

Finite Element Model to Study One Dimensional Calcium Dyanmics in Cardiac Myocytes

Kunal B Pathak
Nirma University
Ahmedabad, Gujarat, India
kunal.pathak@nirmauni.ac.in

Neeru Adlakha
SVNIT, Surat, Gujarat, India
neeru.adlakha21@gmail.com

Published 2 December 2015

The multi physical process involving calcium ions regulate expansion and contraction of cardiac myocytes. This mechanism of expansion and contraction of cardiac myocytes is responsible for contraction and expansion of heart for pumping of blood into arteries and receiving blood into heart from vein. Thus calcium dynamics in cardiac myocytes is responsible for the activities of the myocytes cells and functioning of the heart. The specific spatiotemporal calcium ion dynamics is required to trigger, sustain and terminate activity of the cell. In this paper an attempt has been done to propose a model to study calcium dynamics in cardiac myocytes for a one-dimensional unsteady state case. The model incorporates the process like diffusion, reaction involving source and excess buffers. Appropriate boundary conditions and initial conditions have been framed. The finite element method has been employed to obtain the solution. The numerical results have been used to study the effect of buffers and source influx on calcium dynamics in cardiac myocytes.

Keywords: Reaction diffusion equation; unsteady state; excess buffers; finite element method.

Mathematics Subject Classification:

1. Introduction

The functioning of heart is achieved through expansion and contraction of cardiac myocytes. This expansion and contraction of myocytes is responsible for pumping of blood from heart to arteries.[15] In order to understand the function of heart, it is crucial to understand the multi physical processes involved in cardiac myocytes. These multi physical processes exert a beautiful coordination to achieve the specific spatiotemporal calcium dynamics required for the function of cardiac myocytes. This beautiful coordination of multi physical process and spatiotemporal calcium

dynamics are still not well understood. Thus there is a need to study the calcium dynamic in Cardiac Myocytes involving these multi physical process.

Chemical reaction and diffusion are central to quantitative computational biology. As Ca^{2+} ions diffuse away from the mouth of voltage gated plasma membrane through Ca^{2+} channels into the cytosolic domain of elevated intracellular Ca^{2+} ion activate proteins associated with neurotransmitter release.[1] These Ca^{2+} domain are formed on the presence of ubiquitous Ca^{2+} binding proteins (Troponin-C) of the pre-synaptic terminal. By binding and releasing free Ca^{2+}, endogenous Ca^{2+} binding proteins and other "Ca^{2+} buffers" determine the range of action of Ca^{2+} ions influence the time course of their effect and facilitate clearance of Ca^{2+1}. The intracellular binding proteins bind with calcium ion which results into the contraction of cardiac myocytes. They maintain the balance of calcium ions through active and passive process.[16]

Attempts are reported in the literature for the study of calcium regulation in neuron cell, astrocyte cell, fibroblast cell, oocyte cell, etc.[3,4,7,9] But very few attempts are reported in the literature for the study of calcium dynamics in myocytes.[1,5,6,8,12] Most of the studies reported on calcium diffusion in myocytes are experimental.[8,11] In the present paper an attempt has been made to propose a model for calcium dynamics in cardiac myocytes in the presence of excess buffers for a one-dimensional unsteady state case. The finite element method has been employed to obtain the solution. The effects of the parameters like source influx and buffers on the calcium diffusion in myocytes have been studied with the help of numerical results.

2. Mathematical Formulation

The calcium kinetics in myocytes is governed by a set of following reaction diffusion equations[12]

$$\mathrm{Ca}^{2+} + B_i \underset{k^-}{\overset{k^+}{\Leftrightarrow}} \mathrm{Ca}B_i \tag{1}$$

where B_i and $\mathrm{Ca}B_i$ are free and bound buffers respectively, and i is an index over buffer species. k_i^+ and k_i^- are association and dissociation rate constants for i respectively. Using mass action kinetic law and Fick's law, the diffusion equations can be stated as[12]:

$$\frac{\partial[\mathrm{Ca}^{2+}]}{\partial t} = D_{\mathrm{Ca}}\nabla^2[\mathrm{Ca}^{2+}] + \sum_i R_i \tag{2}$$

$$\frac{\partial[B_i]}{\partial t} = D_{B_i}\nabla^2[B_i] + R_i \tag{3}$$

$$\frac{\partial[\mathrm{Ca}B_i]}{\partial t} = D_{\mathrm{Ca}B_i}\nabla^2[\mathrm{Ca}B_i] - R_i \tag{4}$$

Here the reaction terms R_i's are given by

$$R_i = -k_i^+[\mathrm{Ca}^{2+}][B_i] + k_i^-[\mathrm{Ca}B_i] \tag{5}$$

where $D_{\mathrm{Ca}}, D_{B_i}, D_{\mathrm{Ca}B_i}$ are diffusion coefficients of free calcium, free buffer and Ca^{2+} bound buffer respectively.

Since Ca^{2+} has molecular weight that is small in comparison to most of Ca^{2+} binding species, the diffusion constant of each mobile buffer is not affected by the binding of Ca^{2+} that is $D_{B_i} = D_{\mathrm{Ca}B_i} = D_i$. Hence Eqs. (3) and (4) give[12]

$$\frac{\partial [B_i]_T}{\partial t} = D_i \nabla^2 [B_i]_T \tag{6}$$

and

$$R_i = -k_i^+ [\mathrm{Ca}^{2+}][B_i] + k_i^- ([B_i]_T - [B_i]) \tag{7}$$

where

$$[B_i]_T = [\mathrm{Ca}B_i] + [B_i] \tag{8}$$

In excess buffer approximation, Eqs. (2)–(5) are simplified by assuming that the concentration of free Ca^{2+} buffer is high enough such that its loss is negligible. There is no sink and source for proteins. The association and dissociation rate constants for the bimolecular association reaction between Ca^{2+} and buffer can be combined to obtain a dissociation constant K_i,[12]

$$K_i = k_i^- / k_i^+ \tag{9}$$

The dissociation constant of the buffer has units of μM and the concentration of Ca^{2+} is necessary to cause 50% of the buffer to be in the Ca^{2+} bound form. Considering the steady state of Eqs. (2)–(4) in the absence of influx gives[15]

$$[B_i]_\infty = \frac{K_i [B_i]_T}{K_i + [\mathrm{Ca}^{2+}]_\infty} \tag{10}$$

and

$$[\mathrm{Ca}B_i]_\infty = \frac{[\mathrm{Ca}^{2+}]_\infty [B_i]_T}{K_i + [\mathrm{Ca}^{2+}]_\infty} \tag{11}$$

where $[\mathrm{Ca}^{2+}]_\infty$ is the "background" or ambient free Ca^{2+} concentration, and $[B_i]_\infty$ and $[\mathrm{Ca}B_i]_\infty$ are the equilibrium concentrations of free and bound buffer with respect to index i. The equation of calcium diffusion becomes[15]

$$\frac{\partial [\mathrm{Ca}^{2+}]}{\partial t} = D_{\mathrm{Ca}} \nabla^2 [\mathrm{Ca}^{2+}] - \sum_i k_i^+ [B_i]_\infty ([\mathrm{Ca}^{2+}] - [\mathrm{Ca}^{2+}]_\infty) \tag{12}$$

The expression (12) for a one dimensional unsteady state case in polar coordinates for individual buffer is given by[16]

$$\frac{1}{D_{\mathrm{Ca}}}\frac{\partial[\mathrm{Ca}^{2+}]}{\partial t} = \frac{1}{r}\frac{d}{dr}\left(r\frac{d[\mathrm{Ca}^{2+}]}{dr}\right) - \frac{k^{+}[B]_{\infty}}{D_{\mathrm{Ca}}}([\mathrm{Ca}^{2+}] - [\mathrm{Ca}^{2+}]_{\infty}) \tag{13}$$

The point source of calcium is assumed at $r = 0\,\mu$m. Thus the appropriate boundary condition can be taken as[13]

$$\lim_{r\to 0}\left(-2\pi D_{\mathrm{Ca}} r\frac{\partial[\mathrm{Ca}^{2+}]}{\partial r}\right) = \sigma_{\mathrm{Ca}} \tag{14}$$

Here an influx of free Ca^{2+} is taken at the rate σ_{Ca} by Faraday's law, $\sigma_{\mathrm{Ca}} = \frac{I_{\mathrm{Ca}}}{zF}$.[13] It is assumed that background concentration of Ca^{2+} is $0.1\,\mu$M is maintained at a position and as it goes far away from the source. The radial distance is considered as finite one i.e., radius of the cell and thus the boundary condition is given by[13]

$$\lim_{r\to 7.8}[\mathrm{Ca}^{2+}] = [\mathrm{Ca}^{2+}]_{\infty} = 0.1\,\mu M \tag{15}$$

The initial concentration at $t = 0\,$s is taken as $0.1\,\mu$M. i.e.,

$$\lim_{t\to 0}[\mathrm{Ca}^{2+}] = 0.1\,\mu M \tag{16}$$

The one dimensional finite element discretization is given by Fig. 1.

Now the finite element method is employed to solve Eq. (13) with boundary conditions (14) and (15). The discretized variational form of Eq. (13) is given by

$$I^{(e)} = \frac{1}{2}\int_{r_i}^{r_j}[J_1^{(e)} + J_2^{(e)} - J_3^{(e)} + J_4^{(e)}]dr - \left[\frac{\sigma_{\mathrm{Ca}}}{2\pi D_{\mathrm{Ca}}}u^{(e)}\right]_{r_i}^{r_j} \tag{17}$$

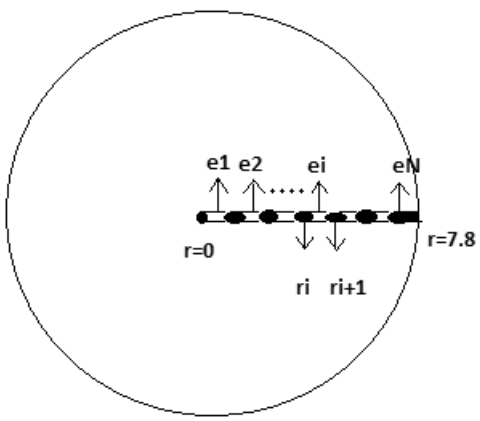

Fig. 1. One dimensional spatial discretization. Here e_i denotes the ith element. And r_i and r_{i+1} denote initial and terminal nodes of ith element.

where

$$J_1^{(e)} = r\left(\frac{\partial u^{(e)}}{\partial r}\right)^2$$

$$J_2^{(e)} = \frac{k^+[B]_\infty}{D_{\mathrm{Ca}}} r u^{(e)2}$$

$$J_3^{(e)} = \frac{2k^+[B]_\infty}{D_{\mathrm{Ca}}} u_\infty u^{(e)} r$$

$$J_4^{(e)} = \frac{r}{D_{\mathrm{Ca}}}\left(\frac{\partial u^{(e)}}{\partial t}\right)^2$$

Here, 'u' is used in lieu of $[\mathrm{Ca}^{2+}]$ for our convenience, $e = 1, 2, \ldots, N$.

The thickness of each element is very small, therefore $u^{(e)}$ is assigned linear variation with respect to position as given by

$$u^{(e)} = C_1 + C_2 r \tag{18}$$

In matrix form Eq. (18) can be written as

$$u^{(e)} = P^T C^{(e)} \tag{19}$$

where

$$P^T = \begin{bmatrix} 1 & r \end{bmatrix} \quad \text{and} \quad C^{(e)} = \begin{bmatrix} C_1 \\ C_2 \end{bmatrix}$$

Also

$$u^{(e)}(r_i) = u_i = C_1 + C_2 r_i \tag{20}$$

$$u^{(e)}(r_j) = u_j = C_1 + C_2 r_j \tag{21}$$

Using Eqs. (19)–(21) we get

$$\bar{u}^{(e)} = P^{(e)} C^{(e)} \tag{22}$$

Where

$$P^{(e)} = \begin{bmatrix} 1 & r_i \\ 1 & r_j \end{bmatrix} \quad \text{and} \quad \bar{u}^{(e)} = \begin{bmatrix} u_i \\ u_j \end{bmatrix}$$

From Eqs. (19) and (22) we get

$$u^{(e)} = P^T R^{(e)} \bar{u}^{(e)} \tag{23}$$

where

$$R^{(e)} = P^{(e)-1} = \frac{1}{r_j - r_i}\begin{bmatrix} r_j & r_i \\ 1 & 1 \end{bmatrix}$$

and r_i and r_j are the boundaries of eth element. Now the integral given in Eq. (17) can also be written as,

$$I^{(e)} = \frac{1}{2}\int_{r_i}^{r_j} r[I_1^{(e)} + I_2^{(e)} + I_3^{(e)} + I_4^{(e)}]dr - \left[\frac{\sigma_{\mathrm{Ca}}}{2\pi D_{\mathrm{Ca}}}\bar{u}^{(e)}\right]_{e=1} \tag{24}$$

where

$$\begin{aligned} I_1^{(e)} &= (P_r^T R^{(e)}\bar{u}^{(e)})^2, \\ I_2^{(e)} &= \frac{k^+[B]_\infty}{D_{\mathrm{Ca}}}(P^T R^{(e)}\bar{u}^{(e)})^2 \\ I_3^{(e)} &= \frac{-2k^+[B]_\infty}{D_{\mathrm{Ca}}}u_\infty(P^T R^{(e)}\bar{u}^{(e)}) \\ I_4^{(e)} &= \frac{1}{D_{\mathrm{Ca}}}\frac{\partial}{\partial t}(P^T R^{(e)}\bar{u}^{(e)})^2 \end{aligned}$$

Now $I^{(e)}$ is minimized with respect to $\bar{u}^{(e)}$

$$\frac{dI^{(e)}}{d\bar{u}^{(e)}} = 0$$

where

$$\bar{u}^{(e)} = [u_i \quad u_j]^T, \quad e = (1, 2, \ldots, N)$$

$$\frac{dI}{d\bar{u}^{(e)}} = \sum_{e=1}^{N} \bar{M}^{(e)}\frac{dI^{(e)}}{d\bar{u}^{(e)}}\bar{M}^{(e)T}$$

$$\bar{M}^{(e)} = \begin{bmatrix} 0 & 0 \\ 1 & 0 \\ 0 & 1 \\ \bullet & \bullet \\ 0 & 0 \end{bmatrix}_{(16\times 2)} \begin{matrix} \\ (i\text{th row}) \\ ((i+1)\text{th row}) \\ \\ \\ \end{matrix} \quad \text{and} \quad I = \sum_{e=1}^{15} I^{(e)}$$

This leads to following system of linear algebraic equations

$$[A]_{(16\times 16)}\frac{d}{dt}[\bar{u}]_{(16\times 1)} + [B]_{(16\times 16)}[\bar{u}]_{(16\times 1)} = [C]_{(16\times 1)} \tag{25}$$

Here, $\bar{u} = [u_1 \quad u2 \quad \bullet \quad \bullet \quad \bullet \quad u_{N+1}]^T$, A and B are system matrices and C is characteristic vector. Crank Nicolson method is employed to solve the system (25). A computer program has been developed in MATLAB 7.10 for the entire problem and simulated on Core i5 processor with 2.40 GHz processing speed, 64-bit machine with 320 GB memory.

3. Numerical Results and Discussion

The biophysical parameters used for the computation of numerical results are given in Table 1.

Figure 2 shows the concentration of calcium along radial direction at different points of time. It is observed that after 1 s the concentration of calcium decreases rapidly as we are moving away from the source from $r = 0\,\mu$m to $r = 1.56\,\mu$m. Then it approaches to its background concentration $0.1\,\mu$M at $r = 2.54\,\mu$m and remains constant thereafter. Due to buffering process the concentration of calcium drops rapidly initially and then after it approaches to its background concentration. The same behavior is observed after 2 s and 3 s. It is also observed that at $t = 2$ s the calcium concentration rapidly decreases as compared to that at $t = 3$ s. As

Table 1. Numerical values of biophysical parameters.[8]

R	Radius of the cell	$7.8\,\mu$m
I_{Ca}	Amplitude of elemental Ca^{2+} release	1 pA
F	Faraday's constant	96,500 C/mol
Z	Valence of Ca^{2+} ion	2
D_{Ca}	Diffusion coefficient of free Ca^{2+} in cytosol for Troponin C	$780\,\mu\text{m}^2/\text{s}$
$[B_1]_T$	Total concentration for each Ca^{2+} buffer of Troponin C	$70\,\mu$M
k^+	Association rate constant for Ca^{2+} binding of Troponin C	$39\,\mu\text{M}^{-1}\text{S}^{-1}$
k^-	Dissociation rate constant for Ca^{2+} binding of Troponin C	$20\,\text{S}^{-1}$
K	Dissociation constant of Troponin C $= \frac{k_1^-}{k_1^+}$,	$0.51\,\mu$M
$[\text{Ca}]_\infty$	Intracellular free Ca^{2+} concentration at rest	0.1μM

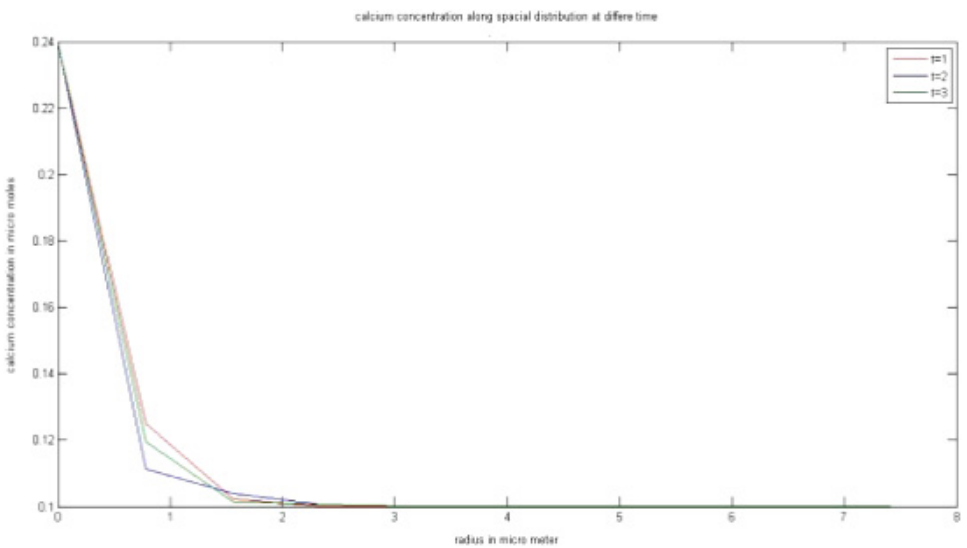

Fig. 2. Calcium concentration along radial direction at different points of time.

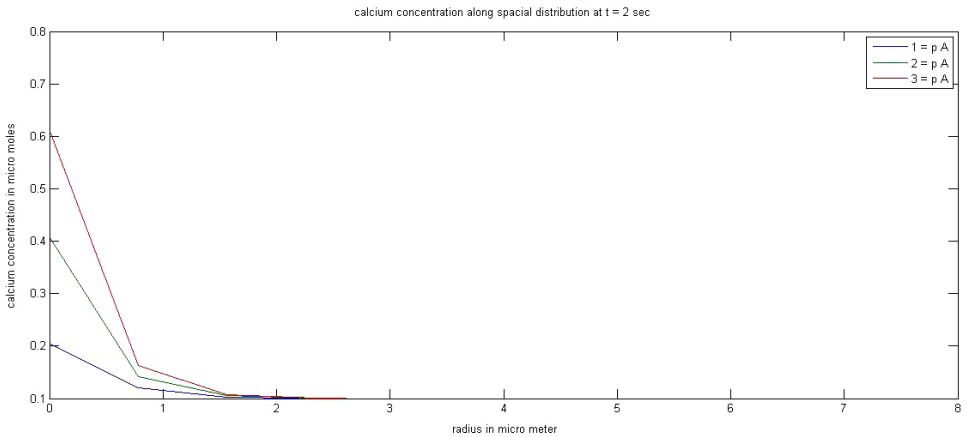

Fig. 3. Calcium concentration along radial direction for different values of source influx at $t = 2\,\mathrm{s}$.

distant increases the calcium concentration achieves its background concentration after $r = 3\,\mu\mathrm{m}$.

Figure 3 shows the calcium concentration at $t = 2\,\mathrm{s}$ for different rates of source influx 1 pA, 2 pA and 3 pA along radial direction. It is observed that the concentration of calcium is decreases rapidly from $r = 0\,\mu\mathrm{m}$ to $r = 1.56\,\mu\mathrm{m}$ and approaches to its background concentration at $r = 2.54\,\mu\mathrm{m}$ for source influx 1 pA, 2 pA and 3 pA. It is also observed that for higher values of source influx the concentration decreases more rapidly compare to low values of source influx. Excess buffer reduce the concentration of calcium at higher values of source influx more rapidly by buffering process. Further the calcium concentration at the source is higher for higher rates of influx and this increase in calcium concentration at source is in the ratio of rates of source influx.

Figure 4 shows the calcium concentration at $t = 2\,\mathrm{s}$ for different buffer concentrations $50\,\mu\mathrm{M}$, $100\,\mu\mathrm{M}$ and $200\,\mu\mathrm{M}$ along radial direction. It is observed that the concentration of calcium decreases rapidly from $r = 0\,\mu\mathrm{m}$ to $r = 1.56\,\mu\mathrm{m}$ and approaches to its background concentration at $r = 2.54\,\mu\mathrm{m}$ for different buffer concentration. It is also observed that for higher values of buffer the calcium concentration decreases more rapidly as compared to that for the low values of buffer.

Figure 5 shows calcium concentration along space and time. The results are obtained for $t = 1, 2$ and $4\,\mathrm{s}$ and for $r = 0, 0.78, 1.56, 2.34$ and $3.12\,\mu\mathrm{m}$. It is observed that at $r = 0\,\mu\mathrm{m}$ the concentration increases from $0.1\,\mu\mathrm{M}$ to $0.24\,\mu\mathrm{M}$ in one second and remain constant for ever due to boundary condition at $r = 0\,\mu\mathrm{m}$. The concentration at $r = 3.12\,\mu\mathrm{m}$ increases with time due to calcium diffusion and there after that it approaches to back ground concentration $0.1\,\mu\mathrm{M}$ as time increases. As we are moving away from the source the very small changes in concentration are observed as time increases. A significant effect of buffer is observed at initial stage. As time increases the effect of buffer is not significant.

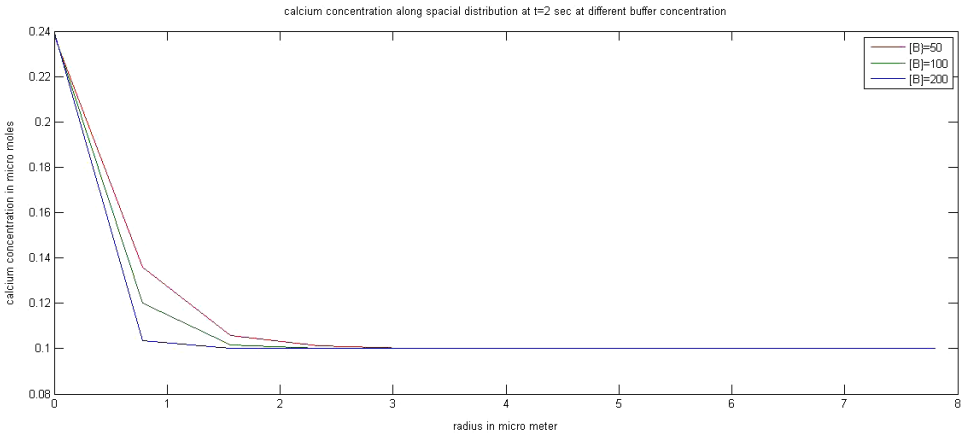

Fig. 4. Calcium concentration along radial direction for different buffer values at $t = 2\,\mathrm{s}$.

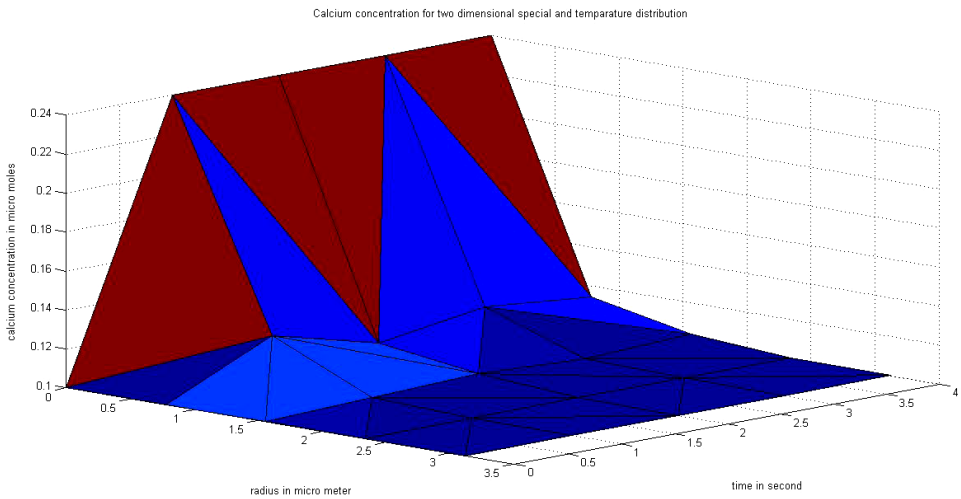

Fig. 5. Spatiotemporal calcium distribution for $\sigma = 1\,\mathrm{pA}$ and $[B] = 70\,\mu\mathrm{M}$.

Figure 6 shows calcium concentration along time for buffer concentrations $50\,\mu\mathrm{M}$, $100\,\mu\mathrm{M}$ and $200\,\mu\mathrm{M}$ at $r = 0.78\,\mu\mathrm{m}$. At buffer concentration $50\,\mu\mathrm{M}$ it is observed that calcium concentration increases from $0.1\,\mu\mathrm{M}$ at $t = 0\,\mathrm{s}$ to $0.1311\,\mu\mathrm{M}$ at $t = 1\,\mathrm{s}$ due to source influx. The concentration of calcium there after decreases from $0.1311\,\mu\mathrm{M}$ from $0.116\,\mu\mathrm{M}$ in a second due to presence of buffers and calcium diffusion. Again the concentration of calcium is increases slightly to $0.1247\,\mu\mathrm{M}$ in a second due to calcium diffusion and decreases to $0.1192\,\mu\mathrm{M}$ in a second. The effect of buffer and diffusion of calcium concentration near the source initially causes oscillations in calcium concentration profiles from $t = 0\,\mathrm{s}$ to $t = 4\,\mathrm{s}$ and thereafter

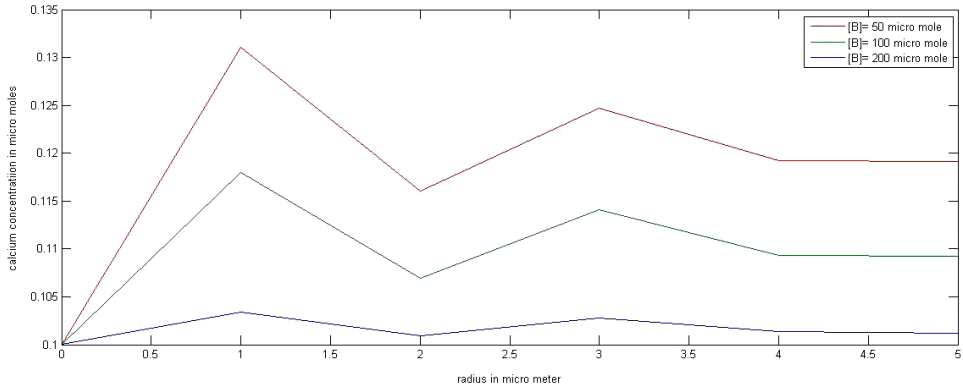

Fig. 6. Calcium concentrations along time for different buffer concentration at $r = 0.78\,\mu$m.

the oscillations disappear indicating that the source influx, buffers and diffusion process have achieved equilibrium or steady state. Similar effect is observed for buffer concentration 100 μM and 200 μM, but the difference is of less magnitude of oscillations of calcium concentration in the cell. The peak calcium concentration is lower for higher buffer concentration. This is due to the fact that the higher buffer concentration binds more calcium to reduce the availability of free calcium concentration in the cell.

Figure 7 shows calcium concentration along time for source influxes 1 PA, 2 PA and 3 PA at $r = 0.78\,\mu$m. At source influx 1 PA it is observed that calcium concentration increases from 0.1 μM at $t = 0$ s to 0.1186 μM at $t = 1$ s due to source influx. The concentration of calcium then after decreases from 0.1186 μM to 0.1084 μM in a second due to presence of buffers. Again the concentration of calcium is increases to 0.1146 μM in a second due to influx and calcium diffusion and decreases to

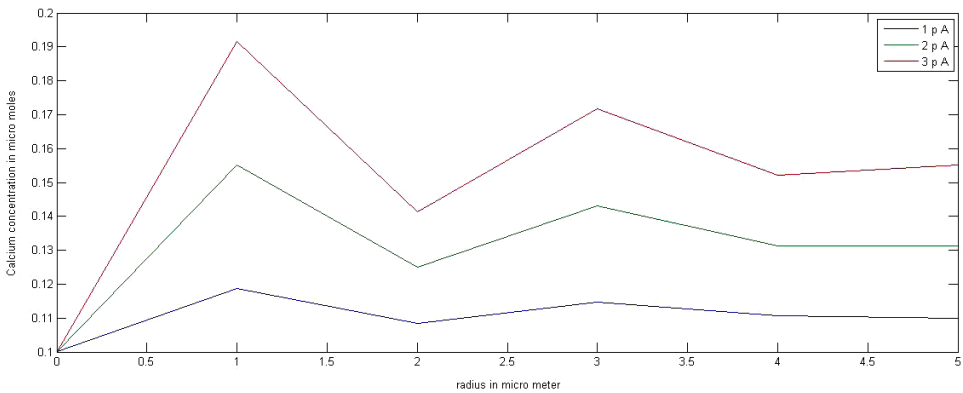

Fig. 7. Calcium concentrations along time for different source influx at $r = 0.78\,\mu$m.

$0.1106\,\mu$M in a second. Similar behavior is observed for higher values of source influx with difference in magnitude of oscillations. It is observed that the peak value of calcium concentration is higher for higher values of influx and is in ratio of the value of the source influx. The source influx has significant effect on calcium concentration profile in the cell. The oscillation of calcium concentration go on decreasing $t = 0\,\text{s}$ to $t = 4\,\text{s}$ and finally disappeared after $t = 5\,\text{s}$. This is due to the steady state achieved by equilibrium of source influx, buffering and diffusion process taking place in the cell in $t = 5\,\text{s}$.

4. Conclusion

A finite element model is proposed and employed to study one-dimensional spatiotemporal calcium distribution in cardiac myocytes involving multi physical process like influx, buffering and diffusion. The model gives us interesting spatiotemporal calcium patterns in relation to the multi physical processes in cell. On the basis of results it is concluded that the calcium concentration in the cell increases in ration of source influx and decreases in the ratio of buffer concentration. In the initial period of time the physical process like influx and buffering causes oscillation in calcium concentration in the cell until the process reached equilibrium state. Thus cardiac myocytes exhibits a beautiful mechanism of well-coordinated effect of multi physical processes like buffering, diffusion and influx. Thus regulating the calcium concentration required for structure and function of the cell. The finite element approach is quite versatile in the present condition of the problem as it gives such flexibility to incorporate theses multi physical process in the model. Such models can be developed further for generating information of spatiotemporal calcium patterns required for contraction and expansion of myocytes which in term is responsible for blood circulation in the body of human. This information can be useful to biomedical scientist for developing protocols for diagnosis and treatment of diseases related to heart. In all it is contribution of new knowledge and new research progression in the field of computational biology.

Acknowledgment

The authors are very thankful to CSIR, New Delhi for providing support to carry out this research.

References

1. P. H. Backx, P. P. De Tonb, H. K. Jurjen, Van Deen, J. M. Barbara, Mulder and D. J. Henke, A model of propagating calcium-induced calcium release mediated by calcium diffusion, *J. Gen. Physiol.* **93** (1989) 963–977.
2. P. A. Naik and K. R. Pardasani, Finite element model to study effect of Na^+/K^+ pump and Na^+/Ca^{2+} exchanger on calcium distribution in Oocytes in presence of buffers, *Asian J. Math. Stat.* **7** (2014) 21–28.

3. A. Jha and N. Adlakha, Finite Element Model to study the effect of excess buffers on calcium dynamics in dendritic spines, *Int. J. Model. Simul. Sci. Comput.* **5** (2013) 1350027.
4. B. K. Jha, N. Adlakha and M. N. Mehta, Finite element model to study calcium diffusion in Astrocyte, *Int. J. Pure Appl. Math.* **7** (2012) 945–955.
5. C. H. Luo and Y. Rudy, A dynamic model of the cardiac ventricular action potential. I Simulations of ionic currents and concentration changes, *Circ. Res.* **74** (1994) 1071–1096.
6. C. H. Luo and Y. Rudy, A dynamic model of the cardiac ventricular action potential. II After depolarization, triggered activity, and potentiation, *Circ. Res.* **74** (1994) 1097–1113.
7. P. Naik and K. R. Pardasani, Finite element model to study effect of buffers in presence of voltage gated Ca^{2+} channels on calcium distribution in Oocytes for one-dimensional unsteady state case, *Int. J. Modern Biol. Med.* (2013) 190–203.
8. A. Michailova, F. Del, M. Egger and E. Niggli, Spatiotemporal features of Ca^{2+} buffering and diffusion in atrail cardiac myocytes with inhibited sarcoplasmic reticulum, *Biophys. J.* **83** (2002) 3134–3151.
9. S. Panday and K. R. Pardasani, Finite element model to study the effect of buffers along with leak form ER on cytosolic Ca^{2+} distribution in Oocyte, **14** (2013) 1–8.
10. J. Post and G. Langer, Sarcolemma Ca^{2+} binding sites in heart: I. Molecular origin in gas dissected, *J. Membr. Biol.* **129** (1992) 49–57.
11. T. R. Shannon, F. Wang, J. Puglisi, C. Weber and D. M. Bers, A mathematical treatment of integrated Ca dynamics within the ventricular myocytes", *Biophys. J.* **87** (2004) 3351–3371.
12. G. D. Smith, J. E. Keizer, M. D. Stern, W. J. Lederer and H. Cheng, A simple numerical model of calcium spark formation and detection in cardiac myocytes, *Biophys. J.* **75** (1998) 15–32.
13. A. Tripathi and N. Adalkha, Finite element to study calcium diffusion in a neuron cell involving JRYR, JSERCA and leak, *J. Appl. Math. Inf.* **31** (2013) 695–709.